### RESEARCH ARTICLE



### Global patterns and drivers of leaf photosynthetic capacity: The relative importance of environmental factors and evolutionary history

Zhengbing Yan<sup>1,2</sup> | Jordi Sardans<sup>3,4</sup> | Josep Peñuelas<sup>3,4</sup> | Matteo Detto<sup>5</sup> | Nicholas G. Smith<sup>6</sup> | Han Wang<sup>7,8</sup> | Lulu Guo<sup>9</sup> | Alice C. Hughes<sup>1</sup> | Zhengfei Guo<sup>1</sup> | Calvin K. F. Lee<sup>1</sup> | Lingli Liu<sup>2,9</sup> | Jin Wu<sup>1,10</sup> |

### Correspondence

Jin Wu, School of Biological Sciences, The University of Hong Kong, Pokfulam Road, Hong Kong Special Administrative Region, China.

Email: jinwu@hku.hk

### **Funding information**

Catalan Government grant, Grant/Award Number: SGR 2017-1005; HKU Seed Fund for Basic Research, Grant/Award Number: 201905159005 and 202011159154; Hong Kong Research Grant Council Early Career Scheme, Grant/Award Number: 27306020; National Natural Science Foundation of China, Grant/Award Number: 31901086, 31922090, DEB-2045968, 32022052 and 31971495; the Fundación Ramon Areces grant, Grant/Award Number: CIVP20A6621; the Spanish Government grants, Grant/Award Number: PID2019-110521GB-I00 and PID2020-115770RB-I00

Handling Editor: Renske E. Onstein

### **Abstract**

Aim: Understanding the considerable variability and drivers of global leaf photosynthetic capacity [indicated by the maximum carboxylation rate standardized to 25°C ( $V_{c,max25}$ )] is an essential step for accurate modelling of terrestrial plant photosynthesis and carbon uptake under climate change. Although current environmental conditions have often been connected with empirical and theoretical models to explain global  $V_{c,max25}$  variability through acclimatization and adaptation, long-term evolutionary history has largely been neglected, but might also explicitly play a role in shaping the  $V_{c,max25}$  variability.

Location: Global.

Time period: Contemporary.

Major taxa studied: Terrestrial plants.

**Methods:** We compiled a geographically comprehensive global dataset of  $V_{c,max25}$  for  $C_3$  plants (n=6917 observations from 2157 species and 425 sites covering all major biomes world-wide), explored the biogeographical and phylogenetic patterns of  $V_{c,max25}$ , and quantified the relative importance of current environmental factors and evolutionary history in driving global  $V_{c,max25}$  variability.

**Results:** We found that  $V_{c,max25}$  differed across different biomes, with higher mean values in relatively drier regions, and across different life-forms, with higher mean values in non-woody relative to woody plants and in legumes relative to non-leguminous

<sup>&</sup>lt;sup>1</sup>Research Area of Ecology and Biodiversity, School of Biological Sciences, The University of Hong Kong, Hong Kong Special Administrative Region, China

<sup>&</sup>lt;sup>2</sup>State Key Laboratory of Vegetation and Environmental Change, Institute of Botany, Chinese Academy of Sciences, Beijing, China

<sup>&</sup>lt;sup>3</sup>CSIC, Global Ecology Unit CREAF-CSIC-UAB, Bellaterra, Spain

<sup>&</sup>lt;sup>4</sup>CREAF, Cerdanyola del Vallès, Spain

<sup>&</sup>lt;sup>5</sup>Department of Ecology and Evolutionary Biology, Princeton University, Princeton, New Jersey, USA

<sup>&</sup>lt;sup>6</sup>Department of Biological Sciences, Texas Tech University, Lubbock, Texas, USA

<sup>&</sup>lt;sup>7</sup>Ministry of Education Key Laboratory for Earth System Modelling, Department of Earth System Science, Tsinghua University, Beijing, China

<sup>&</sup>lt;sup>8</sup>Joint Centre for Global Change Studies, Tsinghua University, Beijing, China

<sup>&</sup>lt;sup>9</sup>College of Life Sciences, University of Chinese Academy of Sciences, Beijing, China

<sup>&</sup>lt;sup>10</sup>Institute for Climate and Carbon Neutrality, The University of Hong Kong, Hong Kong Special Administrative Region, China

plants. The values of  $V_{c,max25}$  displayed a significant phylogenetic signal and diverged in a contrasting manner across phylogenetic groups, with a significant trend along the evolutionary axis towards a higher  $V_{c,max25}$  in more modern clades. A Bayesian phylogenetic linear mixed model revealed that evolutionary history (indicated by phylogeny and species) explained nearly 3-fold more of the variation in global  $V_{c,max25}$  than present-day environment (53 vs. 18%).

**Main conclusions:** These findings contribute to a comprehensive assessment of the patterns and drivers of global  $V_{c,\max 25}$  variability, highlighting the importance of evolutionary history in driving global  $V_{c,\max 25}$  variability, hence terrestrial plant photosynthesis.

#### **KEYWORDS**

biogeography, biome, environmental factor, evolutionary history, global carbon cycling, lifeform, photosynthetic capacity, phylogeny, species

### 1 | INTRODUCTION

Accurate predictions of terrestrial ecosystem responses to global environmental changes require correct modelling of land plant photosynthesis in terrestrial biosphere models (TBMs), the largest carbon flux in the global carbon cycle (Bonan & Doney, 2018; Walker et al., 2021). The amount of carbon assimilated by land plants depends on the interactions between external environmental factors and the intrinsic photosynthetic machinery, which is controlled primarily by the maximum carboxylation rate of the enzyme ribulose-1,5-bisphosphate carboxylase/oxygenase (RuBisCO) in the chloroplasts ( $V_{c,max}$ ; Rogers, Medlyn, et al., 2017). Given that RuBisCO has reached an evolutionarily trapped state, suggested by limited variation in its catalytic activity among phylogenetically distant clades (Bracher et al., 2017), the maximum carboxylation rate standardized to a reference temperature of 25°C (V<sub>c,max25</sub>) mainly reflects the amount of RuBisCO enzyme present per leaf area and directly mediates biotic regulation of photosynthetic carbon uptake and interactions with climate from individual plants to large, vegetated landscapes. It is also a key parameter at the heart of many photosynthetic schemes in TBMs (Bernacchi et al., 2013; Farguhar et al., 1980; Kattge et al., 2009; Wang et al., 2020; Wu et al., 2016). Despite its importance, however,  $V_{c,max25}$  is highly dynamic in nature and is influenced by multiple abiotic and biotic factors, such as climate conditions, soil variables and species properties (Ali et al., 2015; Detto & Xu, 2020; Kattge et al., 2009; Smith & Dukes, 2018; Walker et al., 2014). Accurate characterization and understanding of  $V_{c,max25}$  variability thus represent a fundamental step for improving the modelling of plant photosynthesis in TBMs (Bonan & Doney, 2018; Rogers, Medlyn, et al., 2017). Although understanding and predicting  $V_{c,max25}$  variability have received much scientific attention (Ali et al., 2016; Kattge et al., 2009; Peng et al., 2021; Smith et al., 2019), a holistic understanding and assessment of the patterns and drivers of global  $V_{c,max25}$  variability are still needed.

Current environmental conditions have been assimilated into both empirical and theory-based optimality models for interpreting the large-scale  $V_{c,max25}$  variability (Ali et al., 2016; Peng et al., 2021; Prentice et al., 2014; Smith et al., 2019). For example, studies have revealed associations between  $V_{c,max25}$  and present-day temperature, water, light, soil pH and soil nutrients to which plants are subjected across large geographical extents (Luo et al., 2021; Paillassa et al., 2020; Peng et al., 2021). The likely underlying reason is that these environmental factors mediate plant photosynthetic carbon gain and water or nutrient costs for the construction of RuBisCO and thus determine plant investment in  $V_{c,max25}$  (Paillassa et al., 2020; Prentice et al., 2014; Wang et al., 2020). These empirical observations motivated subsequent theoretical explorations of  $V_{c max 25}$  variability relying on environmental factors, such as the eco-evolutionary optimality theory, which established that plants optimize their  $V_{c,max25}$ to adapt to their living environment to maximize photosynthetic carbon gain (Ali et al., 2016; Jiang et al., 2020; Smith et al., 2019). Moreover, environmental factors could affect  $V_{c,max25}$  variability indirectly by filtering species occurrences and driving biotic competition among species, which, in turn, feeds back to plant nitrogen (N) uptake and other processes related to plant photosynthesis (Kattge et al., 2009; Smith & Dukes, 2018). Through these processes, V<sub>c max 25</sub> has been found to differ considerably across vegetated biomes and life-forms (Ali et al., 2015; Kattge et al., 2009; Luo et al., 2021; Smith & Dukes, 2018). Despite recent progress in elucidating the patterns and factors responsible for large-scale  $V_{\rm c,max25}$  variability, current environmental conditions are generally considered to be the major independent variables to explain global site-mean  $V_{\rm c,max25}$  variability, with the predictive power often found to be low to moderate (Ali et al., 2016; Luo et al., 2021; Peng et al., 2021; Smith et al., 2019). Thus, it remains unclear whether other factors related to plants themselves also play an important role in shaping the large-scale  $V_{c,max25}$  variability.

One candidate, yet underexplored, factor of  $V_{c,max25}$  variability is the evolutionary history of plants; that is, the complex

and long-term product of evolutionary processes resulting from natural selection over time (Cavender-Bares et al., 2016; Peñuelas et al., 2019; Sardans et al., 2021). These evolutionary processes according to the time-scale can be simplified by phylogeny and species. The phylogenetic term accounts for the variability in shared ancestry (i.e., the ancient adaptation and differentiation from other clades), whereas the species term accounts for the interspecific variability independent of the shared ancestry, mostly attributable to recent processes of evolutionary convergence and divergence not yet incorporated into the long-term evolutionary separation among taxonomic clades (Sardans et al., 2021; Vallicrosa, Sardans, Maspons, Zuccarini, et al., 2022). The evolutionary history and the current environmental conditions have contributed to the distribution of modern biomes (Cavender-Bares et al., 2016) and can leave an imprint on plant photosynthetic traits, such as the maximum leaf photosynthetic rate (Flexas & Carriquí, 2020; Gago et al., 2019; Huang et al., 2022; Liu et al., 2022). Meanwhile, evolutionary history has been demonstrated to explain 84%-94% of the large-scale variability in leaf N and phosphorus (P) concentrations (Sardans et al., 2021; Vallicrosa, Sardans, Maspons, & Peñuelas, 2022; Vallicrosa, Sardans, Maspons, Zuccarini, et al., 2022), both of which are essential components of RuBisCO and directly correlated with V<sub>c.max25</sub> (Bahar et al., 2017; Walker et al., 2014). Also, there is empirical evidence that genotypes and phylogeny can alter RuBisCO kinetic parameters (Galmes et al., 2015; Jump & Peñuelas, 2005). All together, these accumulated clues suggest that evolutionary history might be a key and fundamental factor in driving the global variability in  $V_{c,max25}$ , but the phylogenetic structure of V<sub>c max25</sub> and the relative importance of current environmental factors and evolutionary history in shaping the  $V_{c,max25}$  variability on a global scale remain largely unknown.

The aim of this study was to explore biogeographical patterns and phylogenetic structure of  $V_{\rm c,max25}$  on a global scale and to carry out a comprehensive assessment of the relative roles of current environmental factors and long-term evolutionary history in explaining the global  $V_{\rm c,max25}$  variability. Specifically, we ask the following three questions:

- 1. What are the patterns of  $V_{c,max25}$  variation across vegetated biomes and life-forms?
- Does V<sub>c,max25</sub> have a phylogenetic signal and vary across phylogenetic groups?
- 3. What is the relative importance of environmental factors and evolutionary history in shaping global  $V_{c,max25}$  variability?

We address these questions by testing the following hypotheses: (1)  $V_{c,max25}$  could vary across different vegetated biomes and life-forms, with higher values in grasslands relative to shrublands and forests and in fast-growing relative to slow-growing species, because the former plant types usually have higher nutrient concentrations that are often related to more investment

in photosynthetic apparatus (Ali et al., 2016; Kattge et al., 2009; Smith & Dukes, 2018); (2) V<sub>c max25</sub> could show a significant phylogenetic signal, given that  $V_{c,max25}$  has been connected previously with multiple biotic factors (i.e., RuBisCO kinetic parameters and photosynthesis-associated leaf nutrient concentrations) that all display strong phylogenetic regulation (Galmes et al., 2015; Huang et al., 2022; Jump & Peñuelas, 2005; Liu et al., 2022; Sardans et al., 2021); and (3) the global patterns of  $V_{c,max/25}$  could be regulated jointly by both current environmental factors and long-term evolutionary history, with the latter being the dominant driver, because mounting evidence suggests a more important contribution of species identity information to the variability of photosynthesis-associated leaf nutrient concentrations than environmental factors (Asner et al., 2014; Dahlin et al., 2013; Palacio et al., 2022; Sardans et al., 2021; Vallicrosa, Sardans, Maspons, & Peñuelas, 2022; Vallicrosa, Sardans, Maspons, Zuccarini, et al., 2022). To test these three hypotheses, we first collated a global dataset of field-measured  $V_{\rm c.max25}$  for  ${\rm C_3}$  plants with concurrent measurements of present-day environmental factors (i.e., climate and soil variables), then integrated this unique global dataset with multiple statistical modelling analyses detailed below.

### 2 | MATERIALS AND METHODS

## 2.1 | Field dataset of $V_{c,max25}$ , climate and soil variables

A geographically comprehensive global dataset of  $V_{c,max25}$  for  $C_3$ plants was compiled from three different sources, including one data record from three contrasting forest ecosystems in China (Yan et al., 2021) and two global datasets compiled by Smith et al. (2019) and Peng et al. (2021), respectively. The two global datasets were derived mainly from earlier compilations from different authors or open data sources, including Atkin et al. (2015), Bahar et al. (2017), Bloomfield et al. (2019), Cernusak et al. (2011), Domingues et al. (2010, 2015), Ellsworth and Crous (2016), Keenan and Niinemets (2016), Maire et al. (2015), Niinemets et al. (2015), Rogers, Serbin, et al. (2017), Serbin et al. (2015), Smith and Dukes (2017), Togashi, Atkin, et al. (2018), Togashi, Prentice, et al. (2018), Walker et al. (2014), Wang et al. (2018), Xu et al. (2021), Yan et al. (2021) and the TRY plant trait database (https://www.try-db.org/TryWeb/dp.php). In this newly compiled global  $V_{c,max}$  dataset, we retained only those records with concurrent measurements of leaf temperature. With  $V_{\rm c.max}$  derived at its measurement temperature ( $T_{\rm obs}$ , in degrees Celsius), or  $V_{\rm c,maxTobs}$ , we then calculated  $V_{c,max}$  at 25°C ( $V_{c,max25}$ ), using a modified Arrhenius function (Equations 1 and 2) that describes the instantaneous response of enzyme kinetics to any given temperature (Kattge & Knorr, 2007), as follows:

$$V_{c,\text{max}25} = V_{c,\text{max}T_{\text{obs}}} \times f(T_{\text{obs}}, 25), \tag{1}$$

where

$$f(\mathsf{T}_{\text{obs}}, 25) = e^{\frac{H_a(25 - \mathsf{T}_{\text{obs}})}{298.15R(\mathsf{T}_{\text{obs}} + 273.15)}} \times \frac{1 + e^{\frac{(\mathsf{T}_{\text{obs}} + 273.15)}{R(\mathsf{T}_{\text{obs}} + 273.15)}}}{1 + e^{\frac{298.156 - \mathsf{H}_d}{298.15R}}}$$
(2)

where  $H_{\rm d}$  is the deactivation energy (200,000 J mol<sup>-1</sup>),  $H_{\rm a}$  is the activation energy (71,513 J mol<sup>-1</sup>), R is the universal gas constant (8.314 J mol<sup>-1</sup> K<sup>-1</sup>), and  $\Delta S$  is an entropy term (in joules per mole per kelvin) calculated following Kattge and Knorr (2007):

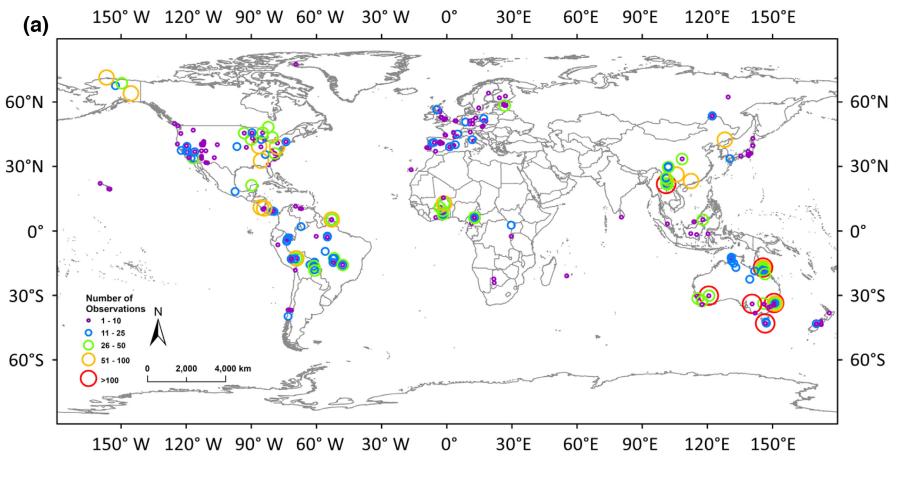
$$\Delta S = -1.07 \times T_{g} + 668.39, \tag{3}$$

where  $T_{\rm g}$  is the mean growing-season temperature as defined below. All the records in this dataset were reported to be measured from natural vegetation, with 6917 measurements from 2157 species and 425 sites, covering all major biomes world-wide (Figure 1). In addition, all these  $V_{\rm c,max}$  measurements were accompanied by corresponding records of present-day climate and soil variables.

Our dataset had six climate variables, namely temperature, precipitation, incoming photosynthetically active radiation (PAR), vapour pressure deficit (VPD), atmospheric  $CO_2$  concentration ( $C_a$ ) and elevation (an indicator of atmospheric pressure). We chose these six climate variables owing to their empirical or theoretical links to  $V_{c,max25}$  variability as explored previously (Ali et al., 2015; Jiang et al., 2020; Peng et al., 2021; Smith et al., 2019; Smith &

Dukes, 2018). Specifically, at each site, temperature, precipitation, PAR and VPD were calculated using the average values across the full growing season, which was defined as all the months with mean monthly air temperature >0°C. These four climate variables were extracted using the corresponding coordinates of each site from monthly data for 1901-2015 at 0.5° resolution provided by the Climatic Research Unit (CRU TS4.01) climatology data (Harris et al., 2014). The values for  $C_2$  were extracted mostly from original records in the databases but approximated using the corresponding values from global average estimates by the NASA GISS model (https://data.giss.nasa.gov/modelforce/ghgases/) when C2 records were lacking in some cases. Elevation was mostly extracted from original records in the databases but was estimated using the extracted values from data at .5° resolution from the WFDEI meteorological forcing dataset (Weedon et al., 2014) when elevation records were lacking in some cases. Temperature and precipitation were interpolated three-dimensionally to the actual site locations (i.e., latitude, longitude and elevation) using geographically weighted regression following Peng et al. (2021). PAR and VPD were calibrated to the site-specific elevation following Smith et al. (2019).

In addition, our dataset had 10 soil variables, namely carbon (C) concentration, N concentration, C:N ratio, cation exchange capacity (CEC), silt concentration, clay concentration, sand concentration, bulk density, pH, and the ratio of actual evapotranspiration to equilibrium evapotranspiration [Priestley-Taylor coefficient ( $\alpha$ )] as an indicator



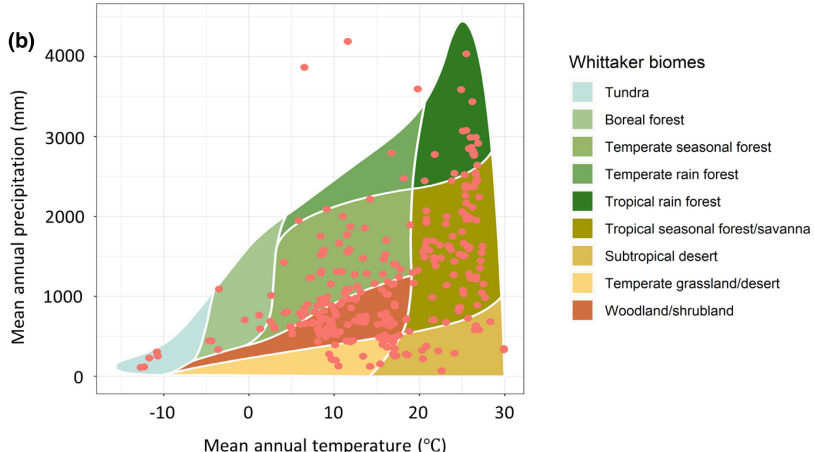


FIGURE 1 Site distribution of the newly compiled field-measured maximum carboxylation rate standardized to 25°C ( $V_{c,max25}$ ) dataset (n=6917 records from 425 sites) for  $C_3$  plants world-wide. (a) Location of each sampling site on the background of a world map. Points of different colours and sizes indicate sites with different numbers of observations. (b) Location of each sampling site superimposed upon classic Whittaker biome classification by climate.

of plant-available surface moisture. These 10 variables reflected soil physical and chemical properties comprehensively and were chosen primarily owing to their apparent correlations with large-scale variability in plant photosynthetic traits (Maire et al., 2015; Paillassa et al., 2020; Peng et al., 2021; Prentice et al., 2014; Smith et al., 2019). The value of  $\alpha$  at each site was calculated at the .5° resolution with the SPLASH model run at a monthly time-scale (Davis et al., 2017). Other soil variables were extracted using the corresponding coordinates of each site from a 250-m resolution global data at the top 30cm depth provided by the ISRIC SoilGrids database (https://soilgrids.org/).

### 2.2 | Classification of the types of biomes and life-forms

To explore the biogeographical patterns of global  $V_{\rm c,max25}$  variability, we analysed the variability of  $V_{\rm c,max25}$  across different biomes. Following the criteria of the classic Whittaker biome classification system based on mean annual precipitation and mean annual temperature (Whittaker, 1975), all our study sites were grouped into nine biomes: tundra, boreal forest, temperate seasonal forest, temperate rain forest, tropical rain forest, tropical seasonal forest/savanna, subtropical desert, temperate grassland/desert and woodland/shrubland.

To explore the change in  $V_{c,max25}$  across different life-forms, we first verified the scientific names of each species against The World Checklist of Vascular Plants (https://www.gbif.org/dataset/f382f Oce-323a-4091-bb9f-add557f3a9a2) and The Leipzig Catalogue of Vascular Plants (https://idiv-biodiversity.github.io/lcvplants/), and identified the plant functional group for each species according to the following literature: the TRY plant trait database (https://www. try-db.org/TryWeb/Home.php) (Kattge et al., 2011), the Flora of China (http://frps.eflora.cn/), Useful Tropical Plants (http://tropi cal.theferns.info/), Australian Native Plants (https://www.anbg. gov.au/index.html) and Wikipedia (https://en.wikipedia.org/wiki). Afterwards, we categorized species into woody or non-woody (i.e., herbaceous) species and legume or non-leguminous plants. The woody species were categorized further into broadleaved or coniferous species and evergreen or deciduous species, whereas the non-woody species were categorized further into perennial (including biennial species) or annual species and forb or graminoid species.

### 2.3 | Statistical analysis

All the statistical analyses were conducted using R code (for details, see Supporting Information Method S1).

## 2.3.1 | Cross-comparison of $V_{c,max25}$ variability across different biomes and life-forms

Following Han et al. (2005), we characterized the biogeographical patterns of  $V_{c, max 25}$  across different biomes using data at the

site–species level (i.e., the averaged  $V_{\rm c,max25}$  for each species within the same sampling site) and explored the change in  $V_{\rm c,max25}$  across different life-forms using data at the species level (i.e., the averaged  $V_{\rm c,max25}$  for each species). We assessed the normality of the  $V_{\rm c,max25}$  distribution with the Shapiro–Wilk test using the software platform R v.4.0.5 (R Development Core Team, 2021) and found that a  $\log_{10}$ -transformation improved the normality of  $V_{\rm c,max25}$ . Therefore, differences among different biomes or life-forms for the  $\log_{10}$ -transformed  $V_{\rm c,max25}$  were determined using one-way ANOVA, with the least significant difference post-hoc test.

### 2.3.2 | Phylogenetic analysis of V<sub>c.max25</sub>

To characterize the phylogenetic structure of  $V_{c,max25}$ , two levels of analyses were conducted at the species level. First, we calculated the phylogenetic signal (i.e., Pagel's λ), which indicates the strength of trait convergence within lineages resulting from stabilizing selection and environmental constraints (Münkemüller et al., 2012). A phylogenetic tree was constructed using the R package "V.PhyloMaker" based on an available mega-phylogeny of vascular plants (Jin & Qian, 2019). We calculated Pagel's  $\lambda$  using the phylosig function from the R package "phytools" based on the variance in phylogenetically independent contrasts relative to tip shuffling randomization (Revell, 2012). We chose Pagel's  $\lambda$  as the phylogenetic signal because it can discriminate between complex models of trait evolution and provide a reliable measurement of effect size (Münkemüller et al., 2012). In addition, Pagel's  $\lambda$  is not sensitive to the number of species in the phylogeny and is suitable for large phylogenies with >50 species (or taxa) (Felsenstein, 1985).

Second, we cross-compared the variability in  $V_{c,max25}$  among different phylogenetic groups. Species were divided into five phylogenetic groups, namely pteridophyte, gymnosperm, magnoliid, monocotyledon and dicotyledon, following the evolutionary time from the oldest to the youngest (Zhang et al., 2020).

# 2.3.3 | Disentangling the relative contribution of environmental factors and evolutionary history to global $V_{c \max 25}$ variability

To explore the separate and joint effects of current environmental factors and evolutionary history on global  $V_{\rm c,max25}$  variability, we performed two analyses at the site–species level, in which the averaged  $V_{\rm c,max25}$  for each species within the same sampling site was used. In the first analysis, we quantified the effects of current environmental factors as a whole on the  $V_{\rm c,max25}$  variability and identified the most important variables. To reduce the impact of multicollinearity among the environmental factors (Supporting Information Figure S1), we retained only the variables with correlation coefficients having absolute values <.7 and a variance inflation factor (VIF) <10 (Doetterl et al., 2015; Supporting Information Table S1). We then used the R package "glmulti" to perform the

model selection for  $V_{\rm c,max25}$  based on the corrected Akaike information criterion (AICc) and evaluated the relative importance of each environmental variable based on the sum of the Akaike weights for the models in which the variable was included. A cutoff relative importance value of .8 was set to differentiate between the important and unimportant variables (Du et al., 2020). We also constructed partial regression plots to illustrate the effect of the sign (positive or negative) of each selected variable on  $V_{\rm c,max25}$  variability, while holding all the other variables constant at their median values, using the R package "visreg" under the "conditional plot" scenario (Breheny & Burchett, 2017; Calcagno & de Mazancourt, 2010; Du et al., 2020).

In the second analysis, we used a Bayesian phylogenetic linear mixed model from the R package "MCMCglmm" to disentangle the relative contributions of current environmental factors and evolutionary history to the global  $V_{c,max25}$  variability. We selected only the most important environmental factors identified above as fixed factors, with the phylogeny and species as random factors. For the phylogeny, we used the phylogenetic tree constructed in Section 2.2 based on an available mega-phylogeny of vascular plants (Jin & Qian, 2019). The random factors described the effect of evolutionary history on  $V_{c,max25}$  variability, with the phylogenetic term accounting for the variability in shared ancestry and the species term accounting for the interspecific variability independent of the shared ancestry (Sardans et al., 2021; Vallicrosa, Sardans, Maspons, & Peñuelas, 2022; Vallicrosa, Sardans, Maspons, Zuccarini, et al., 2022). To examine whether intraspecific variability would affect the Bayesian phylogenetic linear mixed model performance, we performed a sensitivity analysis on the model that was conducted at the individual level (i.e., all original data of  $V_{\rm c.max25}$  from individual observations) or the site-species level (i.e., the averaged V<sub>c max25</sub> for each species within the same sampling site). Our sensitivity analysis demonstrated that the results remained consistent regardless of whether the analysis was at the individual or site-species level. For clarity, we have focused primarily on presenting the data analysis for the Bayesian phylogenetic linear mixed model at the site-species level hereafter.

### 3 | RESULTS

## 3.1 | Patterns of $V_{c,max25}$ across biomes and lifeforms

To investigate the biogeographical patterns of  $V_{\rm c,max25}$ , we cross-compared the  $V_{\rm c,max25}$  variability across different Whittaker biomes and life-forms. Our results showed that  $V_{\rm c,max25}$  varied considerably across biomes, with the mean values being maximum in the subtropical desert and temperate grassland/desert, minimum in the tropical and temperate rain forests, and intermediate in other biomes (i.e., boreal forest, tropical seasonal forest/savanna, tundra, temperate seasonal forest and woodland/shrubland; Figure 2a; Supporting Information Table S1). We also observed large  $V_{\rm c,max25}$  variability

across life-forms, with higher  $V_{\rm c,max25}$  values in non-woody relative to woody plants and in legumes relative to non-legumes (Figure 2b,c; Supporting Information Table S2). Dividing the woody plants into subcategories, we found that deciduous plants had higher  $V_{\rm c,max25}$  relative to evergreen plants and that broadleaved and coniferous plants had no significant difference in  $V_{\rm c,max25}$  (Figure 2d,e; Supporting Information Table S2). Dividing the non-woody plants into subcategories, we found that annuals had significantly higher  $V_{\rm c,max25}$  relative to perennials and that forbs and grasses had no significant difference in  $V_{\rm c,max25}$  (Figure 2f,g; Supporting Information Table S2). Importantly, although the differences in  $V_{\rm c,max25}$  means were sometimes large, there was considerable overlap between the  $V_{\rm c,max25}$  ranges across biomes and life-forms.

### 3.2 | Phylogenetic structure of V<sub>c may 25</sub>

To investigate the phylogenetic structure of  $V_{c,max25}$ , we analysed the phylogenetic signal of  $V_{c,max25}$  and cross-compared the variation in  $V_{c,max25}$  across different phylogenetic groups. We found that  $V_{c,max25}$  showed a significant phylogenetic signal (Pagel's  $\lambda=0.675$ ; p<.001; Figure 3a). This finding was also supported by the significant differences of  $V_{c,max25}$  across the five phylogenetic groups, in which we found that  $V_{c,max25}$  increased from the oldest plants (i.e., pteridophytes) to the youngest plants (i.e., monocotyledons) based on the divergence time (Figure 3b; Supporting Information Table S3). Although broad differences in  $V_{c,max25}$  means certainly existed,  $V_{c,max25}$  space was not divided neatly among different phylogenetic groups.

# 3.3 | Relative contribution of environmental factors and evolutionary history to global $V_{c,max25}$ variability

To investigate the relative importance of environmental factors and evolutionary history in shaping global  $V_{c,max25}$  variability, we first identified the important environmental factors based on the model selection, then conducted a Bayesian phylogenetic linear mixed model to disentangle their separate and joint roles. Seven most important environmental factors were identified to explain a significant proportion of global  $V_{\rm c,max25}$  variability, namely temperature, VPD, elevation, soil silt, soil pH, soil clay and soil bulk density (Figure 4). Partial regression analysis indicated that  $V_{c,max25}$  decreased significantly with temperature, elevation and soil silt content, but increased with VPD, soil pH, soil clay content and soil bulk density (Figure 4). After incorporating these seven environmental factors into the Bayesian model, we found that evolutionary history (indicated by phylogeny and species) outweighed the environmental factors in explaining global  $V_{\rm c,max25}$  variability, with the current environmental factors as a whole explaining only 18.0% of V<sub>c may 25</sub> variance, whereas phylogeny and species explained 31.3 and 21.7% of  $V_{c,max/25}$  variance, respectively (Table 1; Figure 5). In other words,

4668238, 2023, 5, Downlo

com/doi/10.1111/geb.13660 by Texas Tech University Libraries, Wiley Online

Library on [01/09/2023]. See

ons) on Wiley Online Library for rules of use; OA articles are governed by the applicable Creative Commons

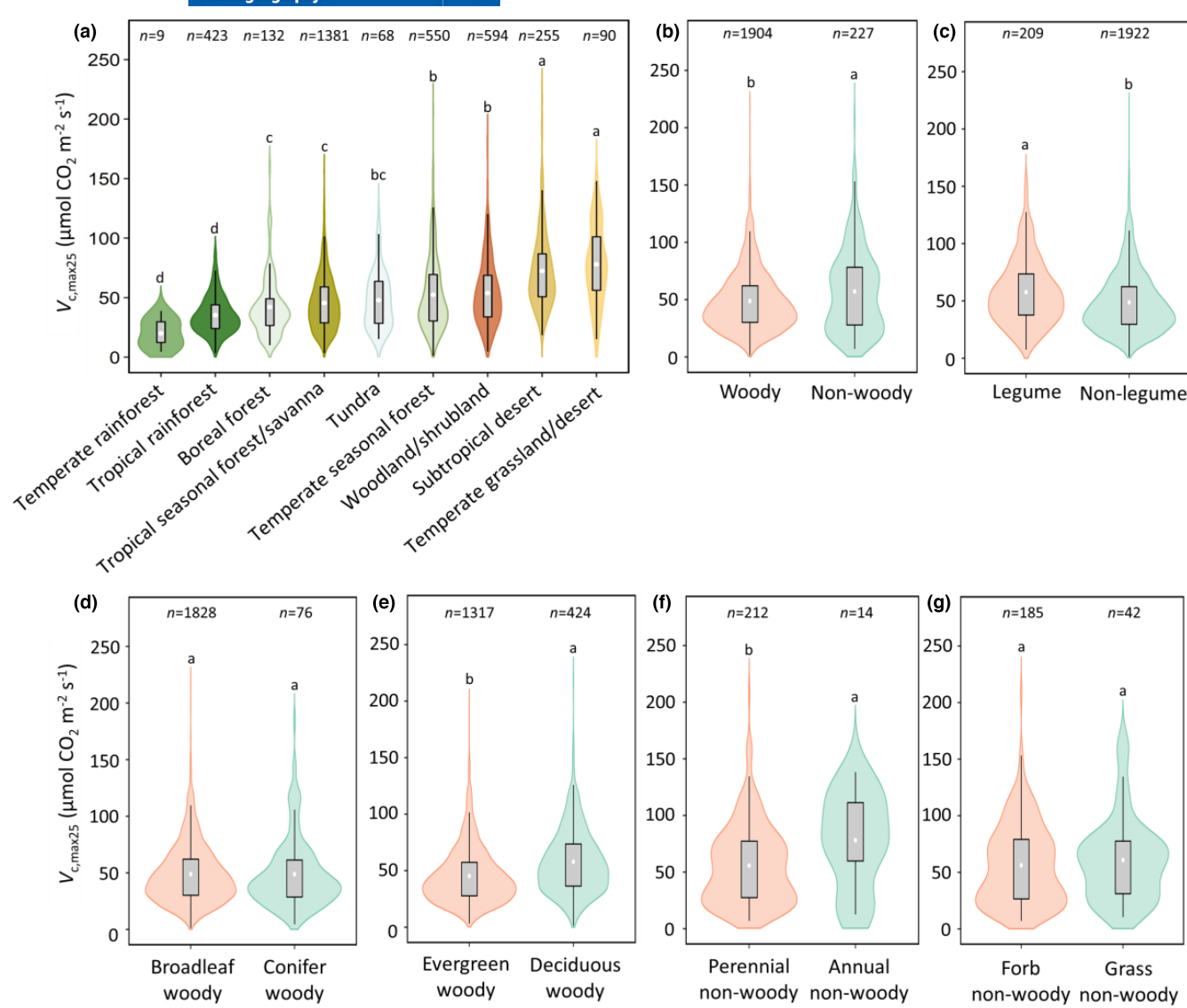


FIGURE 2 Patterns of maximum carboxylation rate standardized to 25°C ( $V_{c,max25}$ ) across different (a) Whittaker biomes and (b-g) lifeforms. The white circles and the boxes within each violin plot show the mean values and the 95% confidence intervals, and the whiskers in each violin plot represent the range. Different lower-case letters adjoining the violin plots indicate the significant difference (p < .05) among different groups for the  $\log_{10}$ -transformed  $V_{c,max25}$  based on one-way ANNOVA with the least significant difference post-hoc test. The patterns of  $V_{c,max25}$  across different biomes and life-forms were analysed at the site-species level (i.e., the averaged  $V_{c,max25}$  for each species within the same sampling site) and the species level (i.e., the averaged  $V_{c,max25}$  for each species), respectively. The number above each violin plot in panel (a) is the number of records for the site-species combinations within that group, and the number above each violin plot in panels (b-g) is the number of species within that group.

evolutionary history had nearly 3-fold more importance (53.0% vs. 18.0%) in explaining the global  $V_{c,max25}$  variability than current environmental factors (Figure 5).

### 4 | DISCUSSION

A deep understanding of the environmental variables and evolutionary history underlying the large-scale variability in  $V_{c,max25}$  can yield critical insights for the development of TBMs that simulate and forecast terrestrial carbon cycling (Rogers, Medlyn, et al., 2017; Walker et al., 2021). However, characterizing the global variability of  $V_{c,max25}$ 

has been challenging, and current approaches provide substantially divergent estimates (Ali et al., 2015; Kattge et al., 2009; Smith & Dukes, 2018). These divergences are likely to be the result of the poor representativeness of existing datasets of field-measured  $V_{c,max25}$  that allows us to understand how  $V_{c,max25}$  varies spatially, across biomes and within taxa. We studied the global variability of  $V_{c,max25}$  based on an unprecedentedly large and geographically comprehensive dataset, with a high degree of variability across Whittaker biomes and life-forms (Figure 2; Supporting Information Tables S1 and S2). This large variability allowed us to explore systematically the biome-specific patterns that were reported based on smaller field-measured datasets. For example, we found higher

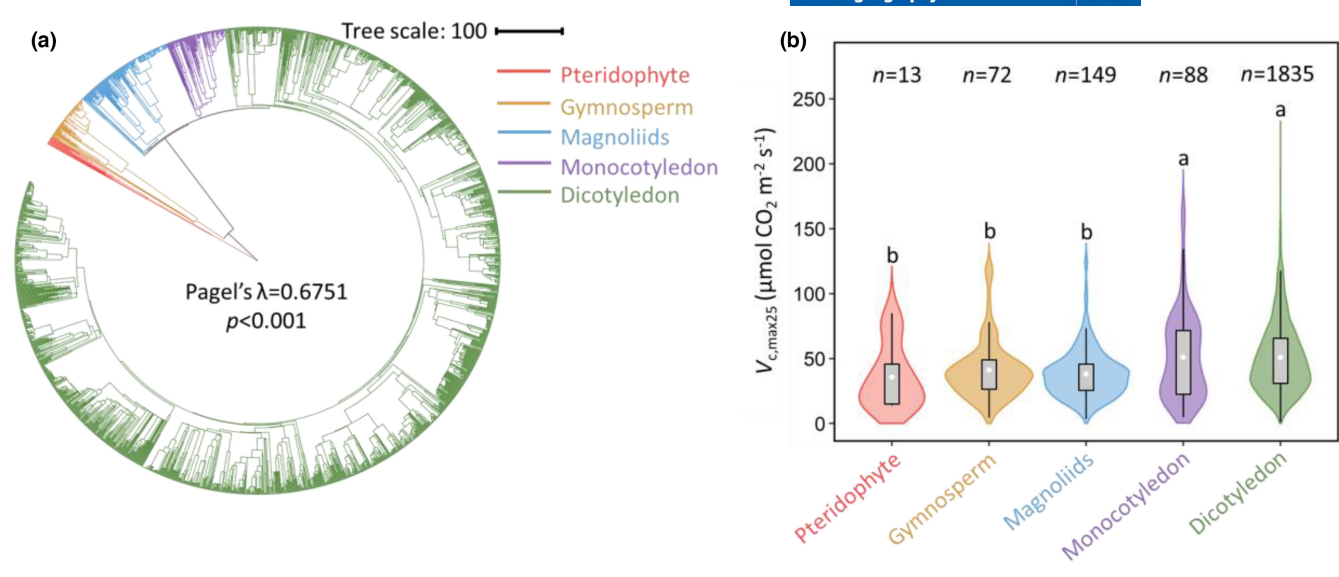


FIGURE 3 Phylogenetic structure of variability in the global maximum carboxylation rate standardized to 25°C ( $V_{c,max25}$ ). (a) Phylogenetic tree of the 2157 species and the phylogenetic signal of  $V_{c,max25}$  indicated by the statistical metric of Pagel's  $\lambda$ . (b) Change in  $V_{c,max25}$  across different phylogenetic groups. The white circles and the boxes within each violin plot show the mean values and the 95% confidence intervals, and the whiskers in each violin plot represent the range. Different lower-case letters adjoining the violin plots indicate the significant difference (p<.05) among different groups for the  $\log_{10}$ -transformed  $V_{c,max25}$  based on one-way ANOVA with the least significant difference post-hoc test. The number above each violin plot is the number of species within that group.

 $V_{c,max25}$  in grasslands relative to shrublands and forests, which was previously reported by Kattge et al. (2009) and Smith et al. (2019). We also found that short-lived, fast-growing species with higher nutrient concentrations and lower leaf mass per area had higher  $V_{c,max25}$  than their long-lived, slow-growing counterparts (Figure 2; Supporting Information Table S2). However, despite significant differences in the mean  $V_{c,max25}$ , variation within each biome and lifeform is too large (Figure 2; Supporting Information Tables S1 and S2) to allow average  $V_{c,max25}$  values to be assigned for use in TBMs (Rogers, Medlyn, et al., 2017) or other practical applications.

What mechanisms cause such a large variability of  $V_{c,max25}$  on a global scale? When the variability explained by phylogeny and species was excluded, we found that the present-day climatic and soil variables altogether explained 18% of this large global  $V_{c,max25}$ variability (Table 1). These current environmental conditions can partly explain some of the observed biome-dependent patterns of  $V_{c.max25}$ . For example, the higher  $V_{c.max25}$  in subtropical desert and temperate grassland/desert relative to tropical and temperate rain forests is explained, in part, by higher VPD, soil pH and soil bulk density (Supporting Information Table S4). These three environmental variables (i.e., VPD, soil pH and soil bulk density) were picked up in the final statistical model of  $V_{c,max25}$  (Figure 4) and could upregulate V<sub>c.max25</sub> owing to their positive effects on the investments in photosynthetic biochemistry (Luo et al., 2021; Maire et al., 2015; Paillassa et al., 2020; Peng et al., 2021). However, current environmental factors were found to have only a low to moderate accumulative predictive power on global  $V_{c,max25}$  variability (Table 1; Smith et al., 2019; Peng et al., 2021), whereas evolutionary history could explain much of the remaining variation (Figure 3; Table 1).

The important role of evolutionary history in explaining global  $V_{c,max25}$  variability is particularly evident from two results (its link with phylogenetic structure, and the higher relative weight of evolutionary history over environmental factors). Our results thus unveil the phylogenetic relatedness of  $V_{c,max25}$  at global scales, expanding previous results that showed the phylogenetic effect on  $V_{c,max25}$ variability at the taxon-specific scale (Huang et al., 2022) and the regional scale (Xu et al., 2021; Yang et al., 2019). This phylogenetic structure of  $V_{c,max25}$  also adds essential information to the patterns of  $V_{c,max25}$  across contrasting biomes with different evolutionary histories. For example, tropical forest biomes are evolutionarily ancient (Ma et al., 2018), whereas shrubland, woodland, grassland and desert biomes are evolutionarily young (Cavender-Bares et al., 2016; Ma et al., 2018). Such differences in evolutionary history seem to support the finding that most late-emerging ecosystems (e.g., woodland/shrubland, subtropical desert and temperate grassland/desert) have higher values of  $V_{c,max25}$  than the early-emerging ecosystems (e.g., tropical rain forest; Figure 2b). In addition, the observed increasing trend of  $V_{c,max25}$  in more modern clades is also consistent with the trend of light-saturated photosynthetic rate ( $A_{max}$ ) over the evolutionary scale (Flexas & Carriquí, 2020; Gago et al., 2019; Huang et al., 2022; Liu et al., 2022). The observed increasing  $V_{c,max25}$  and  $A_{\rm max}$  along plant phylogeny could possibly be explained by the corresponding variation in the fraction of area-based leaf nitrogen concentration (N<sub>a</sub>) allocated to RuBisCO and in leaf structural properties (e.g., mesophyll conductance and cell-wall thickness), both of which are tightly related to leaf photosynthesis (Flexas & Carriquí, 2020; Gago et al., 2019; Huang et al., 2022).

We next investigated the relative importance of environmental factors and evolutionary history in explaining global  $V_{\rm c,max25}$ 

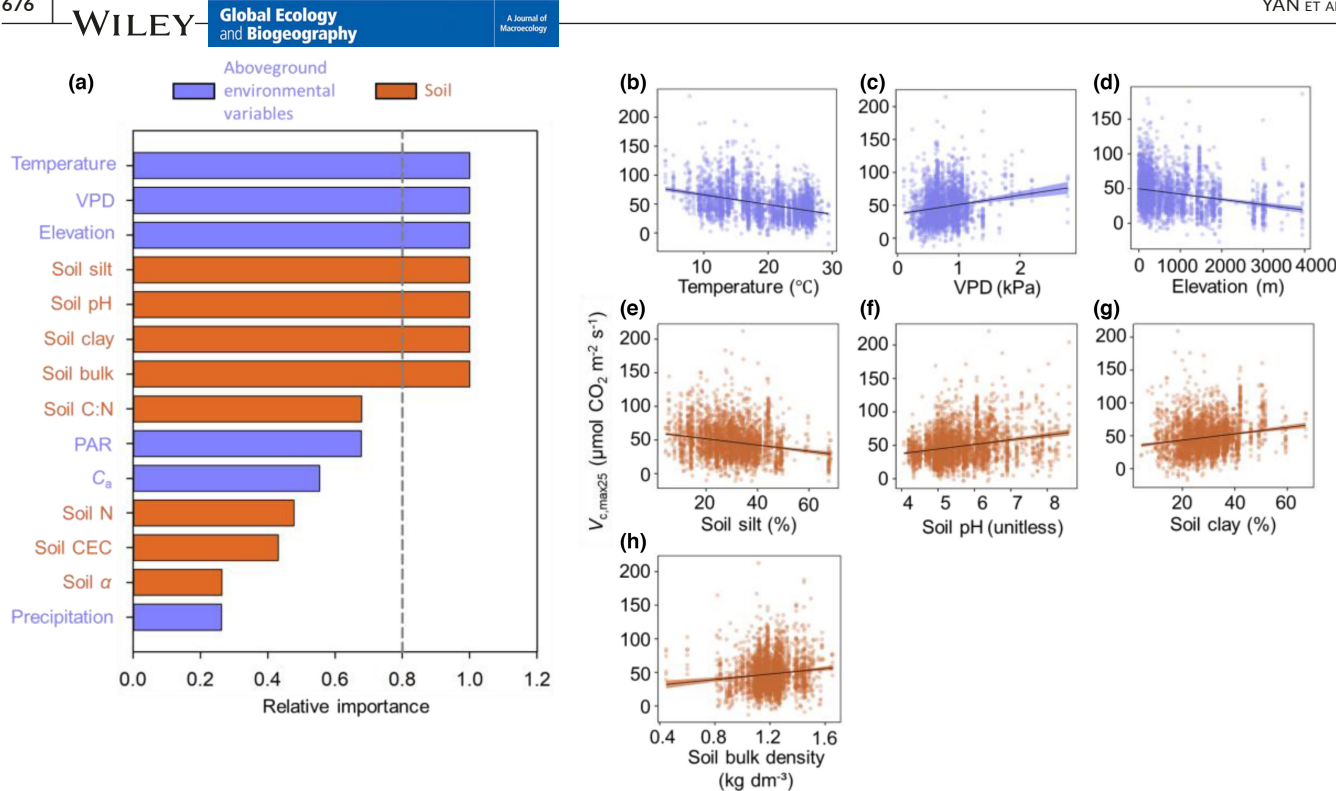


FIGURE 4 Relative importance of environmental factors in predicting the variability in the global maximum carboxylation rate standardized to  $25^{\circ}$ C ( $V_{c,max/5}$ ). (a) The relative importance of each variable is based on the sum of the Akaike weights derived from a model selection using the corrected Akaike information criterion (AICc). (b-h) Partial regression plots of  $V_{c,max25}$  with the predictor of mean growing-season temperature, vapour pressure deficit (VPD), elevation, soil silt content, soil pH, soil clay content and soil bulk density, respectively. The cut-off (dashed line) in panel (a) is set at .8 for identifying the most important predictor variables; the shaded areas in (b-h) are 95% confidential intervals around the predicted relationships. Environmental factors include six aboveground environmental factors [i.e., temperature, VPD, incoming photosynthetically active radiation (PAR), precipitation, atmospheric  $CO_2$  concentration ( $C_2$ ) and elevation] and eight soil variables [i.e., pH, ratio of actual evapotranspiration to equilibrium evapotranspiration (α), clay content, silt content, N content, C:N ratio, bulk density and cation exchange capacity (CEC)].

TABLE 1 Results from Bayesian phylogenetic linear mixed model of maximum carboxylation rate standardized to 25°C at site-species level, with fixed factors (i.e., environmental factors) and random factors (i.e., phylogeny + species) taken into account.

	The statistics of fixed variables						Model
Bayesian model	Variable	Post.mean	Lower 95% CI	Upper 95% CI	Eff.samp	рМСМС	statistics
V <sub>c,max25</sub> T + VPD + Elevation + Silt + pH + Clay + BD + (random = phylogeny + species)	Intercept	-1.1078	-1.6765	4602	1700	.0012	$R_{m}^{2} = .180$
	T	0732	0840	0622	1700	<.0001	$R_{c}^{2} = .710$
	VPD	.6207	.4619	.8081	1444	<.0001	$R_{p}^{2} = .313$
	Elevation	0003	0004	0002	1817	<.0001	$R_{s}^{2} = .217$
	Silt	0134	0167	0100	1700	<.0001	
	рН	.2105	.1557	.2606	1700	<.0001	
	Clay	.0182	.0145	.0222	1962	<.0001	
	BD	.5682	.2791	.8530	1700	<.0001	

Note: The site-species level was analysed by using the averaged  $V_{c,max25}$  for each species within the same sampling site.

Abbreviations: BD, soil bulk density; Clay, soil clay content; pH, soil pH;  $R_c^2$ , percentage of variance explained by all the model (fixed+random);  $R_{\rm m}^2$ , percentage of variance explained by fixed factors;  $R_{\rm p}^2$ , percentage of variance explained by phylogeny;  $R_{\rm s}^2$ , percentage of variance explained by species; Silt, soil silt content; T, mean growing-season temperature;  $V_{c,max25}$ , maximum carboxylation rate standardized to 25°C; VPD, vapour pressure deficit; Post.mean, posterior mean; Eff.samp, the effective sample size; pMCMC, p-value from Monte Carlo sampling by Markov Chain.

variability and found that evolutionary history (represented by both phylogeny and species) explained a much greater proportion than current environmental factors (Table 1). Phylogeny represents long-term evolution together with ancient adaptation and differentiation from other clades, whereas species is linked to more recent evolutionary processes, including strong selection within the

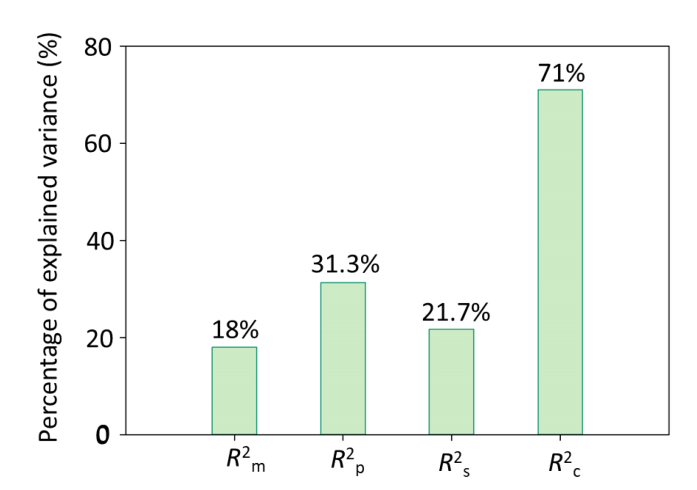


FIGURE 5 Percentage of variance explained by environmental factors and evolutionary history (represented by both phylogeny and species). Abbreviations:  $R_{\rm c}^2$ , percentage of variance explained by both environmental factors and evolutionary history;  $R_{\rm m}^2$ , percentage of variance explained by the seven important environmental factors (Figure 4);  $R_{\rm p}^2$ , percentage of variance explained by phylogeny;  $R_{\rm s}^2$ , percentage of variance explained by species. A Bayesian phylogenetic linear mixed model was used to disentangle the role of different factors in shaping the variability in the global maximum carboxylation rate standardized to 25°C ( $V_{\rm c.max25}$ ) (Table 1).

phylogeny and recent phenotypic/epigenetic shifts that are not directly detectable by phylogenetic information (Sardans et al., 2021; Vallicrosa, Sardans, Maspons, & Peñuelas, 2022; Vallicrosa, Sardans, Maspons, Zuccarini, et al., 2022). Adaptation to different environments in recently separated clades can be linked to a convergent or divergent fast evolution not yet incorporated in the time-scales considered in phylogenetic analyses (Sardans et al., 2021). Thus, previous research, if considering the  $V_{c,max25}$  control only from presentday environmental conditions, often results in very small proportions of  $V_{c,max25}$  variance being explained (Figure 4; Ali et al., 2015; Smith & Dukes, 2018; Peng et al., 2021). This new paradigm could be applied to other plant traits. For example, studies focusing on multi-elemental concentrations and secondary metabolites have also consistently demonstrated the dominant role of evolutionary history in explaining the large-scale variability in various leaf traits (Asner et al., 2014; Palacio et al., 2022; Sardans et al., 2015, 2021; Vallicrosa, Sardans, Maspons, & Peñuelas, 2022; Vallicrosa, Sardans, Maspons, Zuccarini, et al., 2022). Given that both evolutionary history information and current environmental factors jointly regulate large-scale variability in plant functional traits, including  $V_{c,max/25}$ , our results further suggest that the variability stored in the species and phylogeny must be credited, in addition to the site-associated current environmental factors, to estimate and project the global V<sub>c max25</sub> variability accurately. However, it should be noted that the exclusion of species within clades might have major effects on the interpretation of the evolutionary history in shaping  $V_{c,\max 25}$  variability, which should merit further study with a larger dataset including enough data coverage within clades.

In summary, this study revealed, first, that  $V_{\rm c.max25}$  showed significant biogeographical patterns at the global scale and varied remarkably within and across different biomes and life-forms. Second, V<sub>c.max25</sub> exhibited a significant phylogenetic signal, with the evolutionary trend towards higher values in more modern clades. Third, evolutionary history, consisting of both phylogeny and species, largely outperformed present-day environmental conditions in explaining global  $V_{c,max25}$  variability. These results collectively suggest that dynamics related to evolutionary history could be first-order priorities for improving theoretical understanding and modelling of global  $V_{c,max^{25}}$  variability. In addition to the effects of evolutionary history and environmental factors, which together explained 71% of the total variance, there remained a considerable proportion (29%) of unexplained  $V_{c \max 25}$  variability. Some of this unexplained  $V_{c \max 25}$ variability could be attributed to phenological variability in measuring young and old leaves (Albert et al., 2018; Wu et al., 2019), the random measurement and sampling error in our assembled  $V_{c \max 25}$ records (Bloomfield et al., 2018), other unexplored but important environmental factors (e.g., day length, soil moisture, soil available phosphorus concentration; Ali et al., 2015; Maire et al., 2015; Smith & Dukes, 2018) and intraspecific variability at a single site (Bloomfield et al., 2018; Sardans et al., 2021). These warrant more sophisticated investigation through experimental manipulation and field observational approaches across large environmental gradients.

With these results, our work generates at least two insights for mechanistic understanding of global  $V_{c max 25}$  variability and terrestrial biosphere modelling. First, our findings can complement current understanding of the fundamental controls on global  $V_{c,max25}$  variability. Most previous studies considered only the effects of presentday environmental conditions (Ali et al., 2016; Kattge et al., 2009; Peng et al., 2021; Smith et al., 2019) and failed to account for evolutionary history, which displayed a nearly 3-fold higher contribution than present-day environmental factors. The three major factors (i.e., current environment factors, phylogeny and species) that we identified for  $V_{c,max25}$  also provide us with a hypothesized timescale-dependent process in regulating global  $V_{c,max25}$  variability, thus providing a new mechanistic framework for characterizing the variability of  $V_{c,max25}$ , hence plant photosynthesis, across large geographical extents (Rogers, Medlyn, et al., 2017). Given that evolutionary divergence within the same clade or the rate of evolutionary convergence among species from different clades could be increased by recent evolutionary pressures (e.g., climate warming, species migration and shifts in species interactions; Puurtinen et al., 2016; Molina-Montenegro et al., 2018), our findings also imply that global changes might restructure  $V_{c,\max25}$  biogeography not only through plastic responses via direct and short-term environmental effects, but also via changes in species and phylogenetic distributions.

Second, our findings provide critical insights for future work aiming to model  $V_{c,\max25}$  variability. The dominant role of evolutionary history in shaping global  $V_{c,\max25}$  variability provides an important benchmark and theoretical basis for evaluating current  $V_{c,\max25}$  models, including optimality models based on ecoevolutionary first principles (Smith et al., 2019; Wang et al., 2017).

Future studies should explore potential ways to incorporate evolutionary history information mechanistically into the theoretical modelling of  $V_{c,max25}$  and thus better constrain TBMs to improve simulations of terrestrial photosynthesis, carbon cycling and climate change responses (Bonan & Doney, 2018; Walker et al., 2021). This could be helped by leveraging other datasets and models for model integration and benchmarking, such as the Global Biodiversity Information Facility (GBIF) occurrences with globally georeferenced species data, species distribution models (SDMs; Elith & Leathwick, 2009) and the species classification capacity of remotely sensed imaging spectroscopy and laser imaging detection and ranging (LiDAR) techniques (Cavender-Bares et al., 2020). Although challenging, our results indicate that facilitating the inclusion of species and phylogenetic information in large-scale models is greatly needed in the future.

### **ACKNOWLEDGEMENTS**

This work was supported by the National Natural Science Foundation of China (#31922090 and 31901086), the Hong Kong Research Grant Council Early Career Scheme (#27306020) and HKU Seed Fund for Basic Research (#201905159005 and 202011159154). J.S. and J.P. were funded by the Fundación Ramon Areces grant CIVP20A6621, the Spanish Government grants PID2019-110521GB-I00 and PID2020-115770RB-I00, and the Catalan Government grant SGR 2017-1005. J.W. was in part supported by the Innovation and Technology Fund (funding support to State Key Laboratories in Hong Kong of Agrobiotechnology) of the Hong Kong Special Administrative Region, China. M.D. was supported by the Carbon Mitigation Initiative of Princeton University. N.G.S. acknowledges support from the National Science Foundation (DEB-2045968) and Texas Tech University. H.W. acknowledges support from the National Natural Science Foundation of China (#32022052 and 31971495). The authors would like to Mr Yunke Peng for the sharing of globally compiled  $V_{c,max}$  data.

### CONFLICT OF INTEREST STATEMENT

The authors declare no competing interests.

### DATA AVAILABILITY STATEMENT

All the data have been provided in the Supporting Information of the manuscript.

### ORCID

Jordi Sardans https://orcid.org/0000-0003-2478-0219
Nicholas G. Smith https://orcid.org/0000-0001-7048-4387
Lulu Guo https://orcid.org/0000-0003-0067-4630
Lingli Liu https://orcid.org/0000-0002-5696-3151
Jin Wu https://orcid.org/0000-0001-8991-3970

### REFERENCES

Albert, L. P., Wu, J., Prohaska, N., Camargo, P. B., Huxman, T. E., Tribuzy, E. S., Ivanov, V. Y., Oliveira, R. S., Garcia, S., Smith, M. N., Oliveira Junior, R. C., Restrepo-Coupe, N., da Silva, R., Stark, S. C., Martins,

- G. A., Penha, D. V., & Saleska, S. R. (2018). Age-dependent leaf physiology and consequences for crown-scale carbon uptake during the dry season in an Amazon evergreen forest. *New Phytologist*, *219*, 870–884.
- Ali, A. A., Xu, C. G., Rogers, A., Fisher, R. A., Wullschleger, S. D., Massoud, E. C., Vrugt, J. A., Muss, J. D., McDowell, N. G., Fisher, J. B., Reich, P. B., & Wilson, C. J. (2016). A global scale mechanistic model of photosynthetic capacity (LUNA V1. 0). Geoscientific Model Development, 9, 587–606.
- Ali, A. A., Xu, C. G., Rogers, A., McDowell, N. G., Medlyn, B. E., Fisher, R. A., Wullschleger, S. D., Reich, P. B., Vrugt, J. A., Bauerle, W. L., Santiago, L. S., & Wilson, C. J. (2015). Global-scale environmental control of plant photosynthetic capacity. *Ecological Applications*, 25, 2349–2365.
- Asner, G. P., Martin, R. E., Tupayachi, R., Anderson, C. B., Sinca, F., Carranza-Jiménez, L., & Martinez, P. (2014). Amazonian functional diversity from forest canopy chemical assembly. *Proceedings of the National Academy of Sciences of the United States of America*, 111, 5604–5609.
- Atkin, O. K., Bloomfield, K. J., Reich, P. B., Tjoelker, M. G., Asner, G. P., Bonal, D., Bonisch, G., Bradford, M. G., Cernusak, L. A., Cosio, E. G., Creek, D., Crous, K. Y., Domingues, T. F., Dukes, J. S., Egerton, J. J., Evans, J. R., Farquhar, G. D., Fyllas, N. M., Gauthier, P. P., ... Zaragoza-Castells, J. (2015). Global variability in leaf respiration in relation to climate, plant functional types and leaf traits. New Phytologist, 206, 614-636.
- Bahar, N. H. A., Ishida, F. Y., Weerasinghe, L. K., Guerrieri, R., O'Sullivan, O. S., Bloomfield, K. J., Asner, G. P., Martin, R. E., Lloyd, J., Malhi, Y., Phillips, O. L., Meir, P., Salinas, N., Cosio, E. G., Domingues, T. F., Quesada, C. A., Sinca, F., Escudero Vega, A., Zuloaga Ccorimanya, P. P., ... Atkin, O. K. (2017). Leaf-level photosynthetic capacity in low-land Amazonian and high-elevation Andean tropical moist forests of Peru. New Phytologist, 214, 1002–1018.
- Bernacchi, C. J., Bagley, J. E., Serbin, S. P., Ruiz-Vera, U. M., Rosenthal, D. M., & Vanloocke, A. (2013). Modelling  $C_3$  photosynthesis from the chloroplast to the ecosystem. *Plant Cell & Environment*, 36, 1641–1657.
- Bloomfield, K. J., Cernusak, L. A., Eamus, D., Ellsworth, D. S., Prentice, I.
  C., Wright, I. J., Boer, M. M., Bradford, M. G., Cale, P., Cleverly, J.,
  Egerton, J. J. G., Evans, B. J., Hayes, L. S., Hutchinson, M. F., Liddell,
  M. J., Macfarlane, C., Meyer, W. S., Prober, S. M., Togashi, H. F.,
  ... Atkin, O. K. (2018). A continental-scale assessment of variability in leaf traits: Within species, across sites and between seasons.
  Functional Ecology, 32, 1492–1506.
- Bloomfield, K. J., Prentice, I. C., Cernusak, L. A., Eamus, D., Medlyn, B. E., Rumman, R., Wright, I. J., Boer, M. M., Cale, P., Cleverly, J., Egerton, J. J. G., Ellsworth, D. S., Evans, B. J., Hayes, L. S., Hutchinson, M. F., Liddell, M. J., Macfarlane, C., Meyer, W. S., Togashi, H. F., ... Atkin, O. K. (2019). The validity of optimal leaf traits modelled on environmental conditions. New Phytologist. 221, 1409–1423.
- Bonan, G. B., & Doney, S. C. (2018). Climate, ecosystems, and planetary futures: The challenge to predict life in Earth system models. *Science*, *359*, eaam8328.
- Bracher, A., Whitney, S. M., Hartl, F. U., & Hayer-Hartl, M. (2017). Biogenesis and metabolic maintenance of Rubisco. *Annual Review of Plant Biology*, 68, 29–60.
- Breheny, P., & Burchett, W. (2017). Visualization of regression models using visreg. *R Journal*, *9*, 56–71.
- Calcagno, V., & de Mazancourt, C. (2010). glmulti: An R package for easy automated model selection with (generalized) linear models. *Journal of Statistical Software*, 34, 1–29.
- Cavender-Bares, J., Ackerly, D. D., Hobbie, S. E., & Townsend, P. A. (2016). Evolutionary legacy effects on ecosystems: Biogeographic origins, plant traits, and implications for management in the era of global change. Annual Review of Ecology, Evolution, and Systematics, 47, 433–462.

- Cavender-Bares, J., Gamon, J. A., & Townsend, P. A. (2020). Remote sensing of plant biodiversity. Springer Nature.
- Cernusak, L. A., Hutley, L. B., Beringer, J., Holtum, J. A. M., & Turner, B. L. (2011). Photosynthetic physiology of eucalypts along a subcontinental rainfall gradient in northern Australia. Agricultural and Forest Meteorology, 151, 1462-1470.
- Dahlin, K. M., Asner, G. P., & Field, C. B. (2013). Environmental and community controls on plant canopy chemistry in a Mediterraneantype ecosystem. Proceedings of the National Academy of Sciences of the United States of America, 110, 6895-6900.
- Davis, T. W., Prentice, I. C., Stocker, B. D., Thomas, R. T., Whitley, R. J., Wang, H., Evans, B. J., Gallego-Sala, A. V., Sykes, M. T., & Cramer, W. (2017). Simple process-led algorithms for simulating habitats (SPLASH v.1.0): Robust indices of radiation, evapotranspiration and plant-available moisture. Geoscientific Model Development, 10, 689-708.
- Detto, M., & Xu, X. (2020). Optimal leaf life strategies determine V<sub>c.max</sub> dynamic during ontogeny. New Phytologist, 228, 361-375.
- Doetterl, S., Stevens, A., Six, J., Merckx, R., Van Oost, K., Casanova Pinto, M., Casanova-Katny, A., Muñoz, C., Boudin, M., Zagal Venegas, E., & Boeckx, P. (2015). Soil carbon storage controlled by interactions between geochemistry and climate. Nature Geoscience, 8, 780-783.
- Domingues, T. F., Ishida, F. Y., Feldpausch, T. R., Grace, J., Meir, P., Saiz, G., Sene, O., Schrodt, F., Sonké, B., Taedoumg, H., Veenendaal, E. M., Lewis, S., & Lloyd, J. (2015). Biome-specific effects of nitrogen and phosphorus on the photosynthetic characteristics of trees at a forest-savanna boundary in Cameroon. Oecologia, 178, 659-672.
- Domingues, T. F., Meir, P., Feldpausch, T. R., Saiz, G., Veenendaal, E. M., Schrodt, F., Bird, M., Djagbletey, G., Hien, F., Compaore, H., Diallo, A., Grace, J., & Lloyd, J. (2010). Co-limitation of photosynthetic capacity by nitrogen and phosphorus in West Africa woodlands. Plant Cell & Environment, 33, 959-980.
- Du, E. Z., Terrer, C., Pellegrini, A. F. A., Ahlström, A., van Lissa, C. J., Zhao, X., Xia, N., Wu, X. H., & Jackson, R. B. (2020). Global patterns of terrestrial nitrogen and phosphorus limitation. Nature Geoscience, 13, 221-226.
- Elith, J., & Leathwick, J. R. (2009). Species distribution models: Ecological explanation and prediction across space and time. Annual Review of Ecology, Evolution, and Systematics, 40, 677-697.
- Ellsworth, D., & Crous, K. (2016). A global dataset of photosynthetic CO<sub>2</sub> response curves measured in the field at controlled light, CO<sub>2</sub> and temperatures. Western Sydney University. https://doi. org/10.4225/35/569434cfba16e
- Farquhar, G. D., von Caemmerer, S., & Berry, J. A. (1980). A biochemical model of photosynthetic CO<sub>2</sub> assimilation in leaves of C<sub>3</sub> species. Planta, 149, 78-90.
- Felsenstein, J. (1985). Phylogenies and the comparative method. The American Naturalist, 125, 1-15.
- Flexas, J., & Carriquí, M. (2020). Photosynthesis and photosynthetic efficiencies along the terrestrial plant's phylogeny: Lessons for improving crop photosynthesis. The Plant Journal, 101, 964-978.
- Gago, J., Carriquí, M., Nadal, M., Clemente-Moreno, M. J., Coopman, R. E., Fernie, A. R., & Flexas, J. (2019). Photosynthesis optimized across land plant phylogeny. Trends in Plant Science, 24, 947-958.
- Galmes, J., Kapralov, M. V., Copolovici, L. O., Hermida-Carrera, C., & Niinemets, Ü. (2015). Temperature responses of the Rubisco maximum carboxylase activity across domains of life: Phylogenetic signals, trade-offs, and importance for carbon gain. Photosynthesis Research, 123, 183-201.
- Han, W. X., Fang, J. Y., Guo, D. L., & Zhang, Y. (2005). Leaf nitrogen and phosphorus stoichiometry across 753 terrestrial plant species in China. New Phytologist, 168, 377-385.
- Harris, I., Jones, P. D., Osborn, T. J., & Lister, D. H. (2014). Updated high resolution grids of monthly climatic observations-the CRU TS3.10 dataset. International Journal of Climatology, 34, 623-642.

- Huang, G. J., Peng, S. B., & Li, Y. (2022). Variation of photosynthesis during plant evolution and domestication: Implications for improving crop photosynthesis. Journal of Experimental Botany, 73, 4886-4896.
- Jiang, C., Ryu, Y., Wang, H., & Keenan, T. F. (2020). An optimality-based model explains seasonal variation in C<sub>3</sub> plant photosynthetic capacity. Global Change Biology, 26, 6493-6510.
- Jin. Y., & Oian, H. (2019), V.PhyloMaker: An R package that can generate very large phylogenies for vascular plants. Ecography, 42, 1353-1359.
- Jump, A. S., & Peñuelas, J. (2005). Running to stand still: Adaptation and the response of plants to rapid climate change. Ecology Letters, 8, 1010-1020
- Kattge, J., & Knorr, W. (2007). Temperature acclimation in a biochemical model of photosynthesis: A reanalysis of data from 36 species. Plant, Cell & Environment, 30, 1176-1190.
- Kattge, J., Knorr, W., Raddatz, T., & Wirth, C. (2009). Quantifying photosynthetic capacity and its relationship to leaf nitrogen content for global-scale terrestrial biosphere models. Global Change Biology, 15, 976-991.
- Keenan, T. F., & Niinemets, Ü. (2016). Global leaf trait estimates biased due to plasticity in the shade. Nature Plants, 3, 16201.
- Liu, H., Ye, Q., Simpson, K. J., Cui, E. Q., & Xia, J. Y. (2022). Can evolutionary history predict plant plastic responses to climate change? New Phytologist, 235, 1260-1271.
- Luo, X. Z., Keenan, T. F., Chen, J. M., Croft, H., Prentice, C. I., Smith, N. G., Walker, A. P., Wang, H., Wang, R., Xu, C. G., & Zhang, Y. (2021). Global variation in the fraction of leaf nitrogen allocated to photosynthesis. Nature Communications, 12, 1-10.
- Ma, Z. Q., Guo, D. L., Xu, X. L., Lu, M. Z., Bardgett, R. D., Eissenstat, D. M., McCormack, M. L., & Hedin, L. O. (2018). Evolutionary history resolves global organization of root functional traits. Nature, 555, 94-97.
- Maire, V., Wright, I. J., Prentice, I. C., Batjes, N. H., Bhaskar, R., Bodegom, P. M., Cornwell, W. K., Ellsworth, D., Niinemets, Ü., Ordonez, A., Reich, P. B., & Santiago, L. S. (2015). Global effects of soil and climate on leaf photosynthetic traits and rates. Global Ecology and Biogeography, 24, 706-717.
- Molina-Montenegro, M. A., Acuña-Rodríguez, I. S., Flores, T. S. M., Hereme, R., Lafon, A., Atala, C., & Torres-Díaz, C. (2018). Is the causes of plant invasions the result of rapid adaptive evolution in seed traits? Evidence a latitudinal rainfall gradient? Frontiers in Plant Science, 9, 208.
- Münkemüller, T., Lavergne, S., Bzeznik, B., Dray, S., Jombart, T., Schiffers, K., & Thuiller, W. (2012). How to measure and test phylogenetic signal. Methods in Ecology and Evolution, 3, 743-756.
- Niinemets, Ü., Keenan, T. F., & Hallik, L. (2015). A worldwide analysis of within-canopy variations in leaf structural, chemical and physiological traits across plant functional types. New Phytologist, 205, 973-993.
- Paillassa, J., Wright, I. J., Prentice, I. C., Pepin, S., Smith, N. G., Ethier, G., Westerband, A. C., Lamarque, L. J., Wang, H., Cornwell, W. K., & Maire, V. (2020). When and where soil is important to modify the carbon and water economy of leaves. New Phytologist, 228, 121-135.
- Palacio, S., Cera, A., Escudero, A., Luzuriaga, A. L., Sánchez, A. M., Mota, J. F., Perez-Serrano, S. M., Merlo, M. E., Martinez-Hernandez, F., Salmeron-Sanchez, E., Mendoza-Fernandez, A. J., Perez-Garcia, F. J., Montserrat-Marti, G., & Tejero, P. (2022). Recent and ancient evolutionary events shaped plant elemental composition of edaphic endemics. A phylogeny-wide analysis of Iberian gypsum plants. New Phytologist, 235, 2406-2423.
- Peng, Y. K., Bloomfield, K. J., Cernusak, L. A., Domingues, T. F., & Prentice, I. C. (2021). Global climate and nutrient controls of photosynthetic capacity. Communications Biology, 4, 462.
- Peñuelas, J., Fernández-Martínez, M., Ciais, P., Jou, D., Piao, S., Obersteiner, M., Vicca, S., Janssens, I. A., & Sardans, J. (2019).

- The bioelements, the elementome, and the biogeochemical niche. *Ecology*, 100, e02652.
- Prentice, I. C., Dong, N., Gleason, S. M., Maire, V., & Wright, I. J. (2014).
  Balancing the costs of carbon gain and water transport: Testing a new theoretical framework for plant functional ecology. *Ecology Letters*, 17, 82–91.
- Puurtinen, M., Elo, M., Jalasvuori, M., Kahilainen, A., Ketola, T., Kotiaho, J. S., Mönkkönen, M., & Pentikäinen, O. T. (2016). Temperature-dependent mutational robustness can explain faster molecular evolution at warm temperatures, affecting speciation rate and global patterns of species diversity. *Ecography*, *39*, 1025–1033.
- R Development Core Team (2021). R: A language and environment for statistical computing. R Foundation for Statistical Computing.
- Revell, L. J. (2012). Phytools: An R package for phylogenetic comparative biology (and other things). Methods in Ecology and Evolution, 3, 217–223.
- Rogers, A., Medlyn, B. E., Dukes, J. S., Bonan, G., Caemmerer, S., Dietze, M. C., Kattge, J., Leakey, A. D. B., Mercado, L. M., Niinemets, Ü., Prentice, I. C., Serbin, S. P., Sitch, S., Way, D. A., & Zaehle, S. (2017). A roadmap for improving the representation of photosynthesis in Earth system models. *New Phytologist*, 213, 22–42.
- Rogers, A., Serbin, S. P., Ely, K. S., Sloan, V. L., & Wullschleger, S. D. (2017). Terrestrial biosphere models underestimate photosynthetic capacity and CO<sub>2</sub> assimilation in the Arctic. New Phytologist, 216, 1090–1103.
- Sardans, J., Janssens, I. A., Alonso, R., Veresoglou, S. D., Rillig, M. C., Sanders, T. G., Carnicer, J., Filella, I., Farré-Armengol, G., & Peñuelas, J. (2015). Foliar elemental composition of European forest tree species associated with evolutionary traits and present environmental and competitive conditions. Global Ecology and Biogeography, 24, 240-255.
- Sardans, J., Vallicrosa, H., Zuccarini, P., Farré-Armengol, G., Fernández-Martínez, M., Peguero, G., Gargallo-Garriga, A., Ciais, P., Janssens, I. A., Obersteiner, M., Richter, A., & Penuelas, J. (2021). Empirical support for the biogeochemical niche hypothesis in forest trees. Nature Ecology & Evolution, 5, 184–194.
- Serbin, S. P., Singh, A., Desai, A. R., Dubois, S. G., Jablonski, A. D., Kingdon, C. C., Kruger, E. L., & Townsend, P. A. (2015). Remotely estimating photosynthetic capacity, and its response to temperature, in vegetation canopies using imaging spectroscopy. Remote Sensing of Environment, 167, 78–87.
- Smith, N. G., & Dukes, J. S. (2017). LCE: Leaf carbon exchange dataset for tropical, temperate, and boreal species of North and Central America. Ecology, 98, 2978.
- Smith, N. G., & Dukes, J. S. (2018). Drivers of leaf carbon exchange capacity across biomes at the continental scale. *Ecology*, *99*, 1610–1620.
- Smith, N. G., Keenan, T. F., Prentice, I. C., Wang, H., Wright, I. J., Niinemets, Ü., Crous, K. Y., Domingues, T. F., Guerrieri, R., Yoko Ishida, F., Kattge, J., Kruger, E. L., Maire, V., Rogers, A., Serbin, S. P., Tarvainen, L., Togashi, H. F., Townsend, P. A., Wang, M., ... Zhou, S. X. (2019). Global photosynthetic capacity is optimized to the environment. *Ecology Letters*, 22, 506–517.
- Togashi, H. F., Atkin, O. K., Bloomfield, K. J., Bradford, M., Cao, K. F., Dong, N., Evans, B. J., Fan, Z. X., Harrison, S. P., Hua, Z., Liddell, M. J., Lloyd, J., Ni, J., Wang, H., Weerasinghe, L. K., & Prentice, I. C. (2018). Functional trait variation related to gap dynamics in tropical moist forests: A vegetation modelling perspective. Perspectives in Plant Ecology, Evolution and Systematics, 35, 52–64.
- Togashi, H. F., Prentice, I. C., Atkin, O. K., Macfarlane, C., Prober, S. M., Bloomfield, K. J., & Evans, B. J. (2018). Thermal acclimation of leaf photosynthetic traits in an evergreen woodland, consistent with the coordination hypothesis. *Biogeosciences*, 15, 3461–3474.
- Vallicrosa, H., Sardans, J., Maspons, J., & Peñuelas, J. (2022). Global distribution and drivers of forest biome foliar nitrogen to phosphorus ratios (N:P). *Global Ecology and Biogeography*, 31, 861–871.

- Vallicrosa, H., Sardans, J., Maspons, J., Zuccarini, P., Fernández-Martínez, M., Bauters, M., Goll, D. S., Ciais, P., Obersteiner, M., Janssens, I. A., & Penuelas, J. (2022). Global maps and factors driving forest foliar elemental composition: The importance of evolutionary history. New Phytologist, 233, 169–181.
- Walker, A. P., Beckerman, A. P., Gu, L. H., Kattge, J., Cernusak, L. A., Domingues, T. F., Scales, J. C., Wohlfahrt, G., Wullschleger, S. D., & Woodward, F. I. (2014). The relationship of leaf photosynthetic traits-V<sub>cmax</sub> and J<sub>max</sub> to leaf nitrogen, leaf phosphorus, and specific leaf area: A meta-analysis and modeling study. *Ecology and Evolution*, 4, 3218–3235.
- Walker, A. P., De Kauwe, M. G., Bastos, A., Belmecheri, S., Georgiou, K., Keeling, R. F., McMahon, S. M., Medlyn, B. E., Moore, D. J. P., Norby, R. J., Zaehle, S., Anderson-Teixeira, K. J., Battipaglia, G., Brienen, R. J. W., Cabugao, K. G., Cailleret, M., Campbell, E., Canadell, J. G., Ciais, P., ... Zuidema, P. A. (2021). Integrating the evidence for a terrestrial carbon sink caused by increasing atmospheric CO<sub>2</sub>. New Phytologist, 229, 2413–2445.
- Wang, H., Atkin, O. K., Keenan, T. F., Smith, N. G., Wright, I. J., Bloomfield, K. J., Kattge, J., Reich, P. B., & Prentice, I. C. (2020). Acclimation of leaf respiration consistent with optimal photosynthetic capacity. *Global Change Biology*, 26, 2573–2583.
- Wang, H., Harrison, S. P., Prentice, I. C., Yang, Y. Z., Bai, F., Togashi, H. F., Wang, M., Zhou, S. X., & Ni, J. (2018). The China plant trait database: Towards a comprehensive regional compilation of functional traits for land plants. *Ecology*, 99, 500.
- Wang, H., Prentice, I. C., Keenan, T. F., Davis, T. W., Wright, I. J., Cornwell, W. K., Evans, B. J., & Peng, C. H. (2017). Towards a universal model for carbon dioxide uptake by plants. *Nature Plants*, 3, 734–741.
- Weedon, G. P., Balsamo, G., Bellouin, N., Gomes, S., Best, M. J., & Viterbo, P. (2014). The WFDEI meteorological forcing data set: WATCH Forcing Data methodology applied to ERA-Interim reanalysis data. Water Resource Research, 50, 7505–7514.
- Whittaker, R. H. (1975). Communities and ecosystems (p. 385). MacMillan.
  Wu, J., Albert, L. P., Lopes, A. P., Restrepo-Coupe, N., Hayek, M., Wiedemann, K. T., Guan, K. Y., Stark, S. C., Christoffersen, B., Prohaska, N., Tavares, J. V., Marostica, S., Kobayashi, H., Ferreira, M. L., Campos, K. S., da Silva, R., Brando, P. M., Dye, D. G., Huxman, T. E., ... Saleska, S. R. (2016). Leaf development and demography explain photosynthetic seasonality in Amazon evergreen forests. Science, 351, 972-976.
- Wu, J., Rogers, A., Albert, L. P., Ely, K., Prohaska, N., Wolfe, B. T., Oliveira, R. C., Jr., Saleska, S. R., & Serbin, S. P. (2019). Leaf reflectance spectroscopy captures variation in carboxylation capacity across species, canopy environment and leaf age in lowland moist tropical forests. New Phytologist, 224, 663–674.
- Xu, H. Y., Wang, H., Prentice, I. C., Harrison, S. P., & Wright, I. J. (2021). Coordination of plant hydraulic and photosynthetic traits: Confronting optimality theory with field measurements. New Phytologist, 232, 1286–1296.
- Yan, Z. B., Guo, Z. F., Serbin, S. P., Song, G. Q., Zhao, Y. Y., Chen, Y., Wu, S. B., Wang, J., Wang, X., Li, J., Wang, B., Wu, Y., Su, Y., Wang, H., Rogers, A., Liu, L. L., & Wu, J. (2021). Spectroscopy outperforms leaf trait relationships for predicting photosynthetic capacity across different forest types. New Phytologist, 232, 134–147.
- Yang, Y. Z., Wang, H., Harrison, S. P., Prentice, I. C., Wright, I. J., Peng, C. H., & Lin, G. H. (2019). Quantifying leaf-trait covariation and its controls across climates and biomes. New Phytologist, 221, 155–168.
- Zhang, J. H., He, N. P., Liu, C. C., Xu, L., Chen, Z., Li, Y., Wang, R. M., Yu, G. R., Sun, W., Xiao, C. W., Chen, H. Y. H., & Reich, P. B. (2020). Variation and evolution of C:N ratio among different organs enable plants to adapt to N-limited environments. *Global Change Biology*, 26, 2534–2543.

#### **BIOSKETCHES**

Zhengbing Yan is an staff scientist of Institute of Botany, Chinese Academy of Science, with a broad research interest in plant functional ecology, biogeochemical cycles, vegetation spectroscopy and global ecology.

Jin Wu is an assistant professor at the University of Hong Kong, with an interest in ecosystem ecology, plant physiological ecology, climate science, vegetation spectroscopy and earth system science.

#### SUPPORTING INFORMATION

Additional supporting information can be found online in the Supporting Information section at the end of this article.

How to cite this article: Yan, Z., Sardans, J., Peñuelas, J., Detto, M., Smith, N. G., Wang, H., Guo, L., Hughes, A. C., Guo, Z., Lee, C. K. F., Liu, L., & Wu, J. (2023). Global patterns and drivers of leaf photosynthetic capacity: The relative importance of environmental factors and evolutionary history. *Global Ecology and Biogeography*, 32, 668–682. <a href="https://doi.org/10.1111/geb.13660">https://doi.org/10.1111/geb.13660</a>

### **APPENDIX 1**

### **DATA SOURCES**

Atkin, O. K., Bloomfield, K. J., Reich, P. B., Tjoelker, M. G., Asner, G. P., Bonal, D., Bonisch, G., Bradford, M. G., Cernusak, L. A., Cosio, E. G., Creek, D., Crous, K. Y., Domingues, T. F., Dukes, J. S., Egerton, J. J., Evans, J. R., Farquhar, G. D., Fyllas, N. M., Gauthier, P. P., ... Zaragoza-Castells, J. (2015). Global variability in leaf respiration in relation to climate, plant functional types and leaf traits. *New Phytologist*, 206, 614–636.

Bahar, N. H. A., Ishida, F. Y., Weerasinghe, L. K., Guerrieri, R., O'Sullivan, O. S., Bloomfield, K. J., Asner, G. P., Martin, R. E., Lloyd, J., Malhi, Y., Phillips, O. L., Meir, P., Salinas, N., Cosio, E. G., Domingues, T. F., Quesada, C. A., Sinca, F., Escudero Vega, A., Zuloaga Ccorimanya, P. P., ... Atkin, O. K. (2017). Leaf-level photosynthetic capacity in lowland Amazonian and high-elevation Andean tropical moist forests of Peru. *New Phytologist*, 214, 1002–1018.

Bloomfield, K. J., Prentice, I. C., Cernusak, L. A., Eamus, D., Medlyn, B. E., Rumman, R., Wright, I. J., Boer, M. M., Cale, P., Cleverly, J., Egerton, J. J. G., Ellsworth, D. S., Evans, B. J., Hayes, L. S., Hutchinson, M. F., Liddell, M. J., Macfarlane, C., Meyer, W. S., Togashi, H. F., ... Atkin, O. K. (2019). The validity of optimal leaf

traits modelled on environmental conditions. *New Phytologist*, 221, 1409–1423.

Cernusak, L. A., Hutley, L. B., Beringer, J., Holtum, J. A. M., & Turner, B. L. (2011). Photosynthetic physiology of eucalypts along a sub-continental rainfall gradient in northern Australia. *Agricultural and Forest Meteorology*, 151, 1462–1470.

Domingues, T. F., Meir, P., Feldpausch, T. R., Saiz, G., Veenendaal, E. M., Schrodt, F., Bird, M., Djagbletey, G., Hien, F., Compaore, H., Diallo, A., Grace, J., & Lloyd, J. (2010). Co-limitation of photosynthetic capacity by nitrogen and phosphorus in West Africa woodlands. *Plant Cell & Environment*, *33*, 959–980.

Domingues, T. F., Ishida, F. Y., Feldpausch, T. R., Grace, J., Meir, P., Saiz, G., Sene, O., Schrodt, F., Sonké, B., Taedoumg, H., Veenendaal, E. M., Lewis, S., & Lloyd, J. (2015). Biome-specific effects of nitrogen and phosphorus on the photosynthetic characteristics of trees at a forest-savanna boundary in Cameroon. *Oecologia*, 178, 659–672.

Ellsworth, D., & Crous, K. (2016). A global dataset of photosynthetic  $CO_2$  response curves measured in the field at controlled light,  $CO_2$  and temperatures. Western Sydney University. https://doi.org/10.4225/35/569434cfba16e

Kattge, J., Diaz, S., Lavorel, S., Prentice, I. C., Leadley, P., Bonisch, G., Garnier, E., Westoby, M., Reich, P. B., Wright, I. J., Cornelissen, J. H. C., Violle, C., Harrison, S. P., Van Bodegom, P. M., Reichstein, M., Enquist, B. J., Soudzilovskaia, N. A., Ackerly, D. D., Anand, M., ... Wirth, C. (2011). TRY-a global database of plant traits. *Global Change Biology*, *17*, 2905–2935.

Keenan, T. F., & Niinemets, Ü. 2016. Global leaf trait estimates biased due to plasticity in the shade. *Nature Plants*, *3*, 16201.

Maire, V., Wright, I. J., Prentice, I. C., Batjes, N. H., Bhaskar, R., Bodegom, P. M., Cornwell, W. K, Ellsworth, D., Niinemets, Ü., Ordonez, A., Reich, P. B., & Santiago, L. S. (2015). Global effects of soil and climate on leaf photosynthetic traits and rates. *Global Ecology and Biogeography*, 24, 706–717.

Niinemets, Ü., Keenan, T. F. & Hallik, L. (2015). A worldwide analysis of within-canopy variations in leaf structural, chemical and physiological traits across plant functional types. *New Phytologist*, 205, 973–993.

Rogers, A., Serbin, S. P., Ely, K. S., Sloan, V. L., & Wullschleger, S. D. (2017). Terrestrial biosphere models underestimate photosynthetic capacity and  ${\rm CO_2}$  assimilation in the Arctic. *New Phytologist*, 216, 1090–1103.

Serbin, S. P., Singh, A., Desai, A. R., Dubois, S. G., Jablonski, A. D., Kingdon, C. C., Kruger, E. L., & Townsend, P. A. (2015). Remotely estimating photosynthetic capacity, and its response to temperature, in vegetation canopies using imaging spectroscopy. *Remote Sensing of Environment*, 167, 78–87.

Smith, N. G., & Dukes, J. S. (2017). LCE: Leaf carbon exchange dataset for tropical, temperate, and boreal species of North and Central America. *Ecology*, *98*, 2978.

Togashi, H. F., Atkin, O. K., Bloomfield, K. J., Bradford, M., Cao, K. F., Dong, N., Evans, B. J., Fan, Z. X., Harrison, S. P., Hua, Z., Liddell, M. J., Lloyd, J., Ni, J., Wang, H., Weerasinghe, L. K., & Prentice, I. C.

(2018). Functional trait variation related to gap dynamics in tropical moist forests: A vegetation modelling perspective. *Perspectives in Plant Ecology, Evolution and Systematics*, 35, 52–64.

Togashi, H. F., Prentice, I. C., Atkin, O. K., Macfarlane, C., Prober, S. M., Bloomfield, K. J., & Evans B. J. (2018). Thermal acclimation of leaf photosynthetic traits in an evergreen woodland, consistent with the coordination hypothesis. *Biogeosciences*, 15, 3461–3474.

Walker, A. P., Beckerman, A. P., Gu, L. H., Kattge, J., Cernusak, L. A., Domingues, T. F., Scales, J. C., Wohlfahrt, G., Wullschleger, S. D., & Woodward, F. I. (2014). The relationship of leaf photosynthetic traits- $V_{\rm cmax}$  and  $J_{\rm max}$  to leaf nitrogen, leaf phosphorus, and specific leaf area: a meta-analysis and modeling study. *Ecology and Evolution*, 4, 3218–3235.

Wang, H., Harrison, S. P., Prentice, I. C., Yang, Y. Z., Bai, F., Togashi, H. F., Wang, M., Zhou, S. X., & Ni, J. (2018). The China Plant Trait Database: towards a comprehensive regional compilation of functional traits for land plants. *Ecology*, *99*, 500.

Xu, H. Y., Wang, H., Prentice, I. C., Harrison, S. P., & Wright, I. J. (2021). Coordination of plant hydraulic and photosynthetic traits: confronting optimality theory with field measurements. *New Phytologist*, 232, 1286–1296.

Yan, Z. B., Guo, Z. F., Serbin, S. P., Song, G. Q., Zhao, Y. Y., Chen, Y., Wu, S. B., Wang, J., Wang, X., Li, J., Wang, B., Wu, Y., Su, Y., Wang, H., Rogers, A., Liu, L. L., & Wu, J. (2021). Spectroscopy outperforms leaf trait relationships for predicting photosynthetic capacity across different forest types. *New Phytologist*, 232, 134–147.